ACS APPLIED MATERIALS & INTERFACES

Research Article

www.acsami.org

Low-Temperature Fabrication of Mesoporous Solid Strong Bases by Using Multifunction of a Carbon Interlayer

Xiao-Yan Liu, Lin-Bing Sun,* Xiao-Dan Liu, Ai-Guo Li, Feng Lu, and Xiao-Qin Liu*

State Key Laboratory of Materials-Oriented Chemical Engineering, College of Chemistry and Chemical Engineering, Nanjing University of Technology, Nanjing, Jiangsu 210009, China

Supporting Information

ABSTRACT: Mesoporous solid strong bases are highly promising for applications as environmentally benign catalysts in various reactions. Their preparation attracts increasing attention for the demand of sustainable chemistry. In the present study, a new strategy was designed to fabricate strong basicity on mesoporous silica by using multifunction of a carbon interlayer. A typical mesoporous silica, SBA-15, was precoated with a layer of carbon prior to the introduction of base precursor $LiNO_3$. The carbon interlayer performs two functions by promoting the conversion of $LiNO_3$ at low temperatures and by improving the alkali-resistant ability of siliceous host. Only a tiny amount of $LiNO_3$ was decomposed on pristine SBA-15 at 400 °C; for the samples containing >8 wt % of carbon, however, $LiNO_3$ can be entirely converted to strongly basic sites Li_2O under the same conditions. The guest−host redox reaction was proven to be the answer for the conversion of $LiNO_3$, which breaks the tradition of thermally induced decomposition. More importantly, the residual carbon layer can prevent the siliceous frameworks from corroding by the newly formed strongly basic species, which is different from the complete destruction of mesostructure in the absence of carbon. Therefore, materials possessing both ordered mesostructure and strong basicity were successfully fabricated, which is extremely desirable for catalysis and impossible to realize by conventional methods. We also demonstrated that the resultant mesoporous basic materials are active in heterogeneous synthesis of dimethyl carbonate (DMC) and the yield of DMC can reach 32.4%, which is apparently higher than that over the catalysts without a carbon interlayer (<12.9%) despite the same lithium content. The strong basicity, in combination with the uniform mesopores, is believed to be responsible for such a high activity.

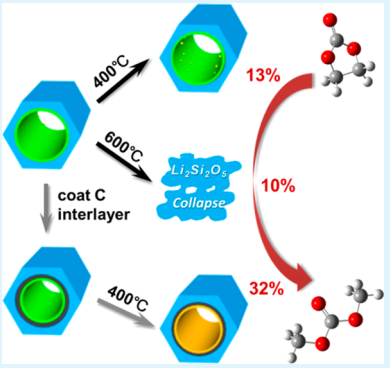

KEYWORDS: *alkali-resistance, basicity generation, carbon interlayer, guest−host redox reaction, mesoporous silica, transesterification*

INTRODUCTION

For the demand of green chemistry and sustainable development, increasing attention has been given to the substitution of conventional homogeneous catalysts with heterogeneous ones. Among heterogeneous catalysts, mesoporous solid strong bases are extremely intriguing for applications in environmentally friendly catalytic processes, because of some obvious advantages such as easy separation, no corrosion, and negligible waste production.[1−4] Their large pore sizes favor mass transfer and avoid deactivation originated from coke formation that commonly happens in microporous catalysts.[5−8] Furthermore, the reactions involving bulky reactants and/or products become possible under the catalysis of mesoporous solid bases. Therefore, great efforts have been dedicated to fabricate mesoporous materials with strong basicity.

New opportunities have been opened up in many areas of chemistry and material science since the discovery of mesoporous silica M41S.[9] A collection of mesoporous materials with various pore structures (e.g., hexagonal, cubic, and lamellar)[10−12] and pore walls composition (e.g., silica, alumina, and zirconia)[13−16] was successfully synthesized by use of templating methods. Among those candidates with mesostructure, mesoporous silica is the best choice of support in theory, due to its low cost, high stability, and good synthetic controllability. By grafting basic organic groups (such as amine groups) onto mesoporous silica, some interesting solid bases with mesostructure can be produced.[17−23] Nonetheless, the basicity stemmed from organic groups is relatively weak. Additionally, degradation of the organic part will take place at elevated temperatures, which limits the application of these organic−inorganic composites to low temperatures (<170 °C). Through treating mesoporous silicas with ammonia or nitrogen, some oxygen atoms in the siliceous frameworks can be displaced by nitrogen atoms, which gives rise to oxynitride frameworks and affords a new kind of solid base with mesostructure.[24−28] However, the temperature for nitrogen incorporation is usually higher than 900 °C, and the strength of resultant basic sites is still low.

To improve the base strength, alkali metal nitrates (e.g., $LiNO_3$ and KNO_3) were employed as base precursors and dispersed on porous supports such as alumina and zirconia.[29−32] Strongly basic oxides can be produced from

Received: July 28, 2013
Accepted: September 10, 2013
Published: September 10, 2013

   dx.doi.org/10.1021/am403033z | ACS Appl. Mater. Interfaces 2013, 5, 9823−9829

nitrates decomposition in the process of subsequent calcination, which offers a facile approach to prepare strong bases and even superbases. Aiming to fabricate strong basicity on mesoporous silica, the introduction of alkali metal nitrates was also tried. Unlike the supports alumina and zirconia, however, the decomposition of nitrate on mesoporous silica is quite difficult. In terms of our previous studies, only a trivial amount of KNO_3 was decomposed on silica, even if the sample was activated at a high temperature of 600 °C.[29,33] A further increase in temperature can result in partial decomposition of KNO_3, but the formed strongly basic species are inevitable to react with siliceous support. As a result, the obtained materials only show weak basicity and the mesostructure is seriously damaged. Despite great efforts, generation of strong basicity on mesoporous silica remains a challenge up to now.

According to previous investigations and a deep analysis, we consider that there are two factors obstructing the fabrication of strong basicity on mesoporous silica. One is the difficulty in conversion of precursor to basic species on silica using the thermal method. The other is the poor alkali-resistant ability of siliceous frameworks; the mesostructure can be destroyed even if strongly basic species were produced. In order to fabricate strong basicity on mesoporous silica, both weaknesses should be overcome.

In the present study, we developed a strategy to fabricate strong basicity on mesoporous silica by using multifunction of a carbon interlayer. Mesoporous silica SBA-15 was first coated with a layer of carbon before the introduction of base precursor $LiNO_3$ (Scheme 1). The carbon interlayer performs two

Scheme 1. Low-Temperature Conversion of $LiNO_3$ and Generation of Strong Basicity on Mesoporous Silica by Using Multifunction of the Carbon Interlayer

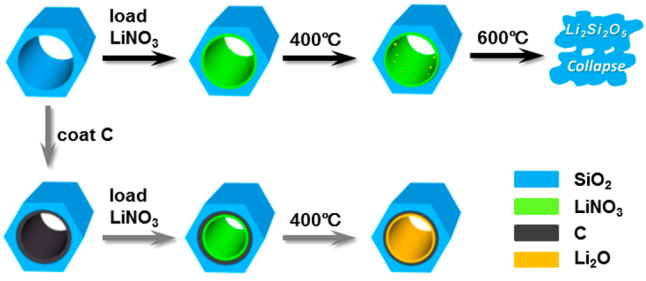

functions by promoting the conversion of $LiNO_3$ and by improving the alkali-resistant ability of siliceous host. It is fascinating that the carbon layer adjusts the surface property and endows the host with reducibility. Strong basicity can thus be generated by taking advantage of the redox interaction between guest and host, which breaks the tradition of thermally induced decomposition. The present strategy greatly declines the treatment temperature, and the conversion of precursor is as high as 100%. More importantly, the residual carbon layer can protect the siliceous frameworks from corrosion by newly generated basic species. As a result, a new type of material owning both ordered mesostructure and strong basicity was successfully constructed, which is extremely desirable for catalysis and improbable to realize by traditional approaches. Characterization of the resultant solid bases was carried out by use of various techniques. The basic catalytic performance of these new materials on transesterification was investigated. On the basis of experimental results, the pathway for generation of strong basicity was proposed as well.

EXPERIMENTAL SECTION

Materials Synthesis. Mesoporous silica SBA-15 was synthesized according to the method reported previously.[10,34,35] Typically, 2 g of Pluronic P123 was first dissolved in 75 g of aqueous HCl solution (1.6 M). Then, 4.25 g of silica source tetraethylorthosilicate (TEOS) was added and stirred at 40 °C for 24 h, followed by hydrothermal treatment at 100 °C for another 24 h. The as-synthesized material was recovered by filtration and dried at ambient conditions. The removal of template was carried out at 550 °C in an air flow for 5 h with a heating ramp of 2 °C·min^{-1}.

The coating of carbon on mesoporous silica was conducted by impregnation of precursor and subsequent carbonization according to the reported method.[36] Furfuryl alcohol (FA) and oxalic acid were used as the carbon precursor and polymerization catalyst, respectively. After evaporation of the solvent ethanol, the resulting solids were polymerized at 80 °C for 2 h under air. Afterward, the composite was heated at 150 °C for 3 h and then evacuated for 1 h in order to remove unreacted FA. Carbonization was carried out at 700 °C for 3 h with a heating rate of 3 °C·min^{-1}. The furnace was purged with a N_2 flow during the carbonization process until the sample was cooled to room temperature. The composition of starting materials was 1 g of SBA-15/x g of FA/0.1x g of oxalic acid/5 g of ethanol (x = 0.05, 0.1, 0.2, and 0.4). Thermogravimetric (TG) analysis showed that the resultant four samples contained 2, 4, 8, and 13 wt % of carbon, and the samples were thus denoted as CS(2), CS(4), CS(8), and CS(13), respectively.

The introduction of base precursor ($LiNO_3$) to supports was performed by wet impregnation. An identical amount of $LiNO_3$ (20 wt %) was used for all samples. In a typical synthesis, 0.2 g of $LiNO_3$ was dissolved in 15 mL of deionized water, followed by addition of 0.8 g of support. After stirring at room temperature for 24 h, the mixture was evaporated at 80 °C and subsequently dried at 100 °C for 4 h. The obtained solids were denoted as LiCS(n) if CS(n) was used as the support, where n represents the content of $LiNO_3$. In a similar process, $LiNO_3$ was directly introduced to SBA-15 and resulted in a reference sample denoted as LiS. To convert supported $LiNO_3$, the solids were calcined at 400 °C (or 600 °C) in a N_2 flow for 3 h, leading to the formation of LiS-T or LiCS(n)-T, where T represents the calcination temperature.

Characterization. X-ray diffraction (XRD) patterns of samples were recorded using a Bruker D8 Advance diffractometer with Cu Kα at 40 kV and 40 mA. Nitrogen adsorption−desorption isotherms were measured using an ASAP 2020 system at −196 °C. The samples were degassed at 300 °C for 4 h before analysis. The Brunauer−Emmett−Teller (BET) surface area was calculated with the relative pressure ranging from 0.04 to 0.20. The total pore volume was derived from the amount adsorbed at the relative pressure of about 0.99. The pore diameter was calculated from the adsorption branch by using Barrett−Joyner−Halenda (BJH) and Kruk−Jaroniec−Sayari (KJS)[37,38] methods. Transmission electron microscopy (TEM) images of the materials were captured in a JEM-2010 UHR electron microscope operated at 200 kV. Fourier transform infrared (IR) spectra of the samples diluted with KBr were performed on a Nicolet Nexus 470 spectrometer with KBr wafer. TG analysis was performed on a thermobalance (STA-499C, NETZSCH). About 10 mg of sample was heated from the room temperature to 800 °C in a flow of N_2 (for the conversion of supported $LiNO_3$) or air (for the analysis of carbon contents).

To measure the amount of basic sites, 100 mg of sample after activation was added into 10 mL of aqueous HCl. The sample suspension was shaken for 24 h, and the slurry was separated by a centrifuge. The remaining acid in liquid phase was titrated with a standard base where phenolphthalein was employed as an indicator. The amount of HCl consumed was used to calculate the basicity.[39−41] Temperature programmed desorption of CO_2 (CO_2-TPD) experiments were conducted on a BELSORP BEL-CAT-A apparatus. The sample was activated at 400 °C (or 600 °C) for 3 h prior to the adsorption of CO_2 at room temperature. After the physical adsorbed CO_2 was purged by a He flow (99.999%) at room temperature, the sample was heated to 900 °C and the CO_2 liberated was detected by a mass spectrometer (HAL201, HIDEN).

Catalytic Test. The obtained basic materials were employed to catalyze the synthesis of dimethyl carbonate (DMC) through the transesterification of ethylene carbonate and methanol. In a typical process, methanol (0.5 mol), ethylene carbonate (0.1 mol), and catalyst (0.5 wt % of methanol) were added to a three-necked glass flask with a water-cooled condenser. All the catalysts were activated at 400 °C (or 600 °C) in a N_2 flow (99.999%) for 3 h prior to reaction. The reaction was conducted at 65 °C with stirring for a given period of time. After the reaction was completed, the reaction mixtures were recovered from the flask and subjected to centrifuging. The obtained upper liquid was then analyzed by gas chromatography (Varian 3800).

RESULTS

Precoating of Carbon Layer on SBA-15. Figure S1, Supporting Information, displays the low-angle XRD patterns of pristine SBA-15 and carbon-coated SBA-15 samples. All of the samples possess an intense diffraction peak accompanied with two weak ones, corresponding to a two-dimensional hexagonal pore regularity. This indicates that the ordered mesostructure is well maintained after the precoating of carbon layer. Figure S2, Supporting Information, presents the N_2 adsorption−desorption results of different samples. The isotherms of carbon-containing samples are of type IV with an H1 hysteresis loop, similar to that of pristine SBA-15. A close inspection shows that the N_2 uptake declines with the increase of carbon content in the samples. As depicted in Figure S3, Supporting Information, a band at 962 cm^{-1} ascribed to the bending vibration of silanols (Si−OH) is observed in the IR spectrum of pristine SBA-15.[42,43] After carbon coating, the band becomes weak and the intensity decreases gradually with the increase of carbon content. This is because of the interaction between carbon layer and siliceous support, which results in the consumption of silanols and the dispersion of carbon on the surface. According the results above, it is clear that that carbon is successfully coated on mesoporous silica and that the ordered mesostructure is well preserved after the introduction of carbon.

Introduction and Conversion of Base Precursor. Aiming to fabricate strong basicity, the base precursor $LiNO_3$ was introduced to the supports. Strong basicity is expected to be generated from the conversion of $LiNO_3$ to Li_2O after activation at certain temperatures. Interestingly, the surface properties of supports have an important effect on the conversion of $LiNO_3$. IR spectra were first employed to characterize the samples before and after activation. As shown in Figure 1, all samples before activation display a sharp band at 1384 cm^{-1} that originates from the asymmetric stretching vibrations of N−O in nitrate.[44] Activation at 400 °C only slightly weakens the band of nitrate in the sample without carbon (i.e., LiS), reflecting the existence of a great deal of residual $LiNO_3$ in the sample. In the case of the samples containing some carbon, namely, LiCS(2) and LiCS(4), however, the intensity of the band at 1384 cm^{-1} declines significantly after activation at the same conditions. Moreover, the intensity of such a band keeps decreasing with the increase of carbon content in the samples. It is worth noting that the characteristic band of nitrate becomes invisible when the carbon content is higher than 8 wt %. That means, $LiNO_3$ is completely converted at 400 °C. On the basis of IR results, it is reasonable that the carbon interlayer greatly promotes the conversion of base precursor $LiNO_3$, and the ratio of converted $LiNO_3$ is strongly dependent on the content of carbon.

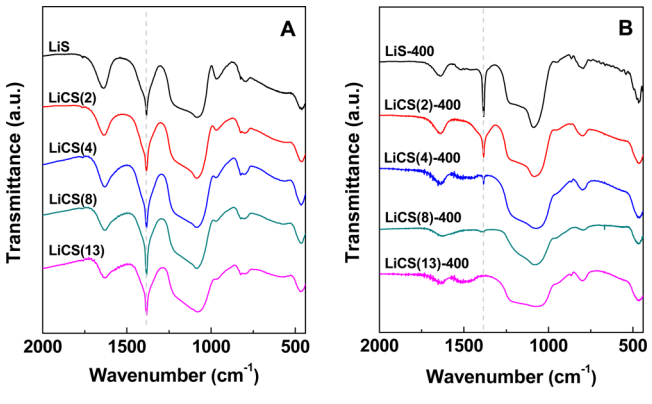

Figure 1. IR spectra of the samples (A) before and (B) after activation.

The promotion of carbon interlayer on the conversion of $LiNO_3$ was further studied by TG. Gaseous products released from the samples in the process of thermal treatment were also monitored by MS. Figure 2 depicts TG curves of typical samples with and without carbon, namely, LiCS(8) and LiS. Both samples give a weight loss centered at around 100 °C ascribed to the desorption of physically adsorbed water. The subsequent weight loss initiated at about 200 °C can be assigned to the conversion of $LiNO_3$. By combining the TG curves with MS results, it can be seen that, on pristine SBA-15, the majority of $LiNO_3$ is decomposed at 570 °C with the minority at 280 °C. Noteworthily, the introduction of a carbon interlayer leads to an apparent decline of conversion temperature from 570 to 430 °C. It is therefore clear that the carbon layer promotes the conversion of $LiNO_3$ at much low temperatures, thus confirming the results from IR.

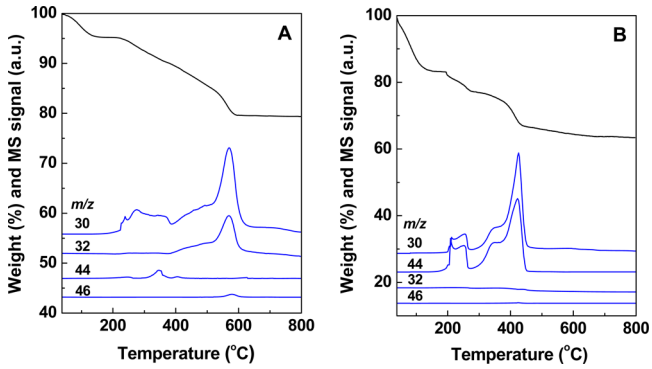

Figure 2. TG curves and MS signals of (A) LiS and (B) LiCS(8) samples.

Figure S4, Supporting Information, displays the wide-angle XRD patterns of the lithium-containing samples before and after activation. Before activation, all of the samples present a broad diffraction peak centered at about 23°, which can be ascribed to amorphous silica walls. After activation at 400 °C, no new phases appeared on the samples. This indicates that lithium species are well dispersed in silica nanopores or the particles of lithium species are too small to give Bragg diffraction.[45] As described above, only a tiny amount of $LiNO_3$ can be decomposed on pristine SBA-15 subjected to activation at 400 °C. To promote the decomposition of $LiNO_3$, a high temperature of 600 °C was also tried in terms of the TG analysis. It is noticeable that some new peaks emerged on LiS-600 despite the low intensity, which can be tentatively attributed to the crystal of $Li_2Si_2O_5$ (JCPDS No. 72-0102).

This suggests that the strongly basic species, which derive from $LiNO_3$ decomposition, react with siliceous frameworks, resulting in the formation of a compound with weak basicity. Actually, the mesostructure of SBA-15 was also destroyed completely as discussed later.

Structural Characteristics of Mesoporous Solid Bases. Structure of the samples after lithium modification was first characterized by low-angle XRD patterns, and the results were illustrated in Figure 3. For the samples containing a carbon interlayer, the diffraction lines ascribed to two-dimensional hexagonal pore symmetry can be well recognized, indicating that the mesostructure is preserved after the formation of basicity. Because most of the $LiNO_3$ were not decomposed on SBA-15 at 400 °C, the diffraction lines in the sample LiS-400 were still visible. When the activation temperature was enhanced to 600 °C, supported $LiNO_3$ can be decomposed. However, all of the diffraction lines disappeared in the sample LiS-600, indicative of the complete destruction of mesostructure due to the poor alkali-resistance of siliceous frameworks.

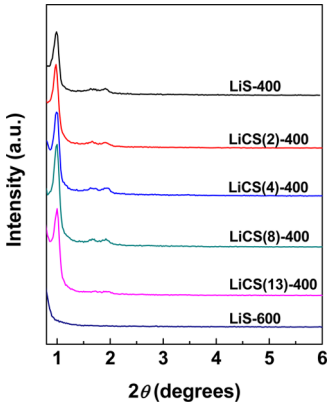

Figure 3. Low-angle XRD patterns of LiS-400, LiCS-400, and LiS-600 samples.

Figure 4 presents N_2 adsorption−desorption isotherms and pore size distributions of different samples. The isotherm of LiS-400 is of type IV with a clear hysteresis loop, implying the mesoporosity of the material. This is because the majority of $LiNO_3$ cannot be decomposed on pristine SBA-15 upon activation at 400 °C. Interestingly, after coating 2 wt % of carbon, the shape of isotherm changed and the hysteresis loop became narrow, which corresponds to a bimodal pore size distribution as shown in Figure 4B. Taking into account that KJS is a more accurate method for pore size analysis, pore size distributions were also calculated by using the KJS method and shown in Figure S5, Supporting Information, and Table 1. As described above, the introduction of 2 wt % of carbon promotes the conversion of $LiNO_3$ to some extent. Nonetheless, the amount of residual carbon is insufficient to protect the siliceous frameworks completely. As a result, the newly formed basic species reacted with siliceous host and partially destructed the mesostructure. For the samples containing >4 wt % of carbon, well-expressed hysteresis loops can be observed, and the shape of hysteresis loop is comparable to the support SBA-15 in the case of samples with a high carbon content. Table 1 lists structural parameters of the samples calculated from N_2 adsorption data. The sample LiS-400 has a high surface area of 351 $m^2 \cdot g^{-1}$ and a pore volume of 0.65 $cm^3 \cdot g^{-1}$, owing to the absence of carbon as well as the decomposition of a negligible amount of $LiNO_3$. The introduction of a small number of carbon results in the decrease of surface areas of samples. With further increase of the carbon content, however, the surface area rises, and the sample LiCS(8)-400 exhibits the largest surface areas among the samples with a carbon interlayer. It is worthy of note that the sample LiS-600 has a pretty low surface area of 33 $m^2 \cdot g^{-1}$, which provides the evidence of the damage of mesostructure.

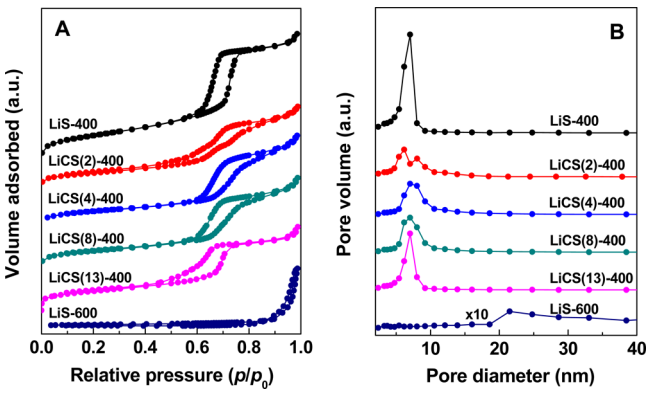

Figure 4. (A) N_2 adsorption−desorption isotherms and (B) pore size distributions calculated by the BJH method of LiS-400, LiCS-400, and LiS-600 samples.

TEM is a useful technique to characterize the ordered structure of mesoporous materials. The images of typical samples were taken and displayed in Figure 5. For the sample after lithium incorporation, that is LiCS(8)-400, the ordered hexagonal arrays of mesopores can be judged from the white dark contrast, which is comparable to the sample CS(8) before lithium introduction. The TEM images thus confirm the results of XRD and N_2 adsorption, indicating the good mesostructure of the resultant solid bases. On the basis of aforementioned results, it is conclusive that the carbon interlayer efficiently prevents the siliceous frameworks from corroding by strongly basic species, and the amount of carbon has an important effect on the maintenance of mesostructure.

Basicity and Catalytic Performance of Mesoporous Solid Bases. The basicity of resultant materials was first characterized by the amount of basic sites. For pristine SBA-15, the amount of basic sites is 0 $mmol \cdot g^{-1}$; coating carbon does not lead to any increase in the amount of basic sites. The samples containing lithium are generally basic while the basicity varies with the carbon content. In the case of LiS-400 and LiS-600 without carbon, the amount of basic sites is only 0.69 and 0.71 $mmol \cdot g^{-1}$ due to incomplete decomposition of $LiNO_3$ and/or the reaction of strongly basic species with silica (Table 1). Interestingly, for the sample containing 2 wt % of carbon, namely, LiCS(2)-400, the amount of basic sites sharply increases to 1.65 $mmol \cdot g^{-1}$. The amount of basic sites keeps rising with the increase of carbon content and reaches 2.87 and 2.86 $mmol \cdot g^{-1}$ for LiCS(8)-400 and LiCS(13)-400, respectively, which is in good agreement with the theoretical value (2.90 $mmol \cdot g^{-1}$) and implies the complete conversion of supported $LiNO_3$ (20 wt %) to basic sites.

The basicity of materials was further determined using CO_2-TPD technique. As presented in Figure 6, the peak of CO_2 desorption on the sample CS(8) is very tiny, if there is any. For the samples containing lithium, the desorption peaks can be tentatively divided into three parts denoted as α, β, and γ at approximately 200, 500, and 700 °C, respectively, which are

dx.doi.org/10.1021/am403033z | ACS Appl. Mater. Interfaces 2013, 5, 9823−9829

Table 1. Physicochemical Properties and Amount of Basic Sites of Different Samples

sample	C content (wt %)[a]	S_{BET} ($m^2 \cdot g^{-1}$)	V_p ($cm^3 \cdot g^{-1}$)	pore size (nm)[b]	amount of basic sites ($mmol \cdot g^{-1}$)[c]
LiS-400	0	351	0.65	8.8	0.69 ± 0.06
LiCS(2)-400	2	176	0.42	6.7/8.8	1.65 ± 0.08
LiCS(4)-400	4	207	0.45	8.8	2.48 ± 0.15
LiCS(8)-400	8	231	0.47	8.1	2.87 ± 0.12
LiCS(13)-400	13	223	0.41	8.1	2.86 ± 0.09
LiS-600	0	33	0.28		0.71 ± 0.07

[a]The content of carbon was measured by TG. [b]Calculated by the KJS method. [c]The amount of basic sites was detected by titration.

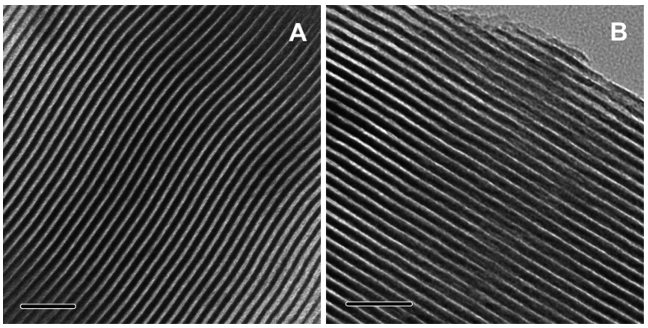

Figure 5. TEM images of (A) CS(8) and (B) LiCS(8)-400 samples. Scale bars represent 50 nm.

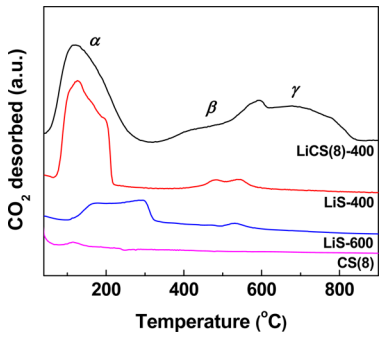

Figure 6. CO_2-TPD profiles of CS(8), LiCS(8)-400, LiS-400, and LiS-600 samples.

tentatively attributed to weak, medium, and strong basicity. Both of the samples LiS-400 and LiS-600 give rise to a major desorption peak ascribed to weakly basic sites, along with a quite minor peak originated from medium basicity. It is worth noting that the sample LiCS(8)-400 containing carbon shows an intense peak caused by strongly basic sites in addition to weak and medium ones. Moreover, the desorption of CO_2 temperature persists up to 810 °C, which is comparable to, if not higher than, some solid superbases,[44,46] thus implying the existence of unusually strong basicity on the material. According to these results, it is obvious that the carbon interlayer is crucial to the fabrication of basicity with regard to both amount and strength of basic sites.

The obtained materials were also applied to the catalytic synthesis of DMC via the transesterification of ethylene carbonate and methanol. As a green chemical, DMC is used as methylating agent in place of dimethyl sulfate and methyl halides, which are toxic and corrosive.[46−48] DMC has also been proposed as carbonylating agent and fuel additive, as well as polar solvent. Traditionally, the synthesis of DMC is carried out in the presence of homogeneous strong bases, while much attention has been given to the development of heterogeneous catalysts recently. As shown in Figure 7, no DMC is produced

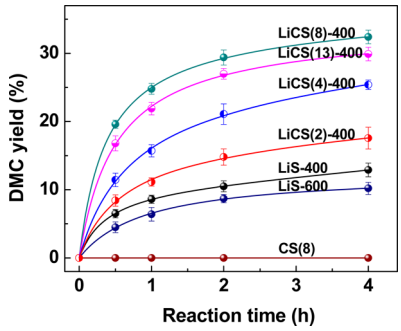

Figure 7. The yield of DMC under the catalysis of different samples.

at all even after the reaction for 4 h over the material without lithium, namely, CS(8). For the materials without carbon, that is LiS-400 and LiS-600, the yield of DMC is 12.9% and 10.2%, respectively. It is interesting to note that the coating of carbon interlayer evidently increases the catalytic activity, and the activity varies with the carbon content in samples. Under the catalysis of LiCS(4)-400 containing 4 wt % of carbon, 25.4% of DMC can be produced. In the case of sample containing 8 wt % of carbon, namely, LiCS(8)-400, the yield of DMC reaches 32.4%, which is apparently superior to the materials LiS-400 and LiS-600 despite an identical lithium content. With a further increase of carbon content to 13 wt %, however, the yield of DMC diminishes slightly. The catalytic performance of materials in the present study was compared with that reported in the literature. It can be found that the yield of DMC is dependent on the type of active sites. Due to the nature of active sites, the activity of catalysts containing Li_2O is generally lower than that derived from Na_2O while higher as compared with MgO.[17,46,49] A reference sample with the same active sites, Li_2O/Al_2O_3, was also prepared by loading Li_2O on the typical support Al_2O_3. Despite the same active sites, the yield of DMC on the present catalyst LiCS(8)-400 (32.4%) is obviously higher than Li_2O/Al_2O_3 (18.8%). In terms of these results, it is safe to say that the catalytic activity of different samples correlates well with their basicity as well as mesostructure. After reaction, regeneration of the spent catalyst LiCS(8)-400 is conducted. The yield of DMC over the regenerated catalyst can still reach 30.1%. That means, most catalytic capacity of the used catalyst can be recovered.

DISCUSSION

The introduction of neutral salt precursors to porous hosts offers a facile method to prepare solid strong bases. Such a method has also been attempted to generate strongly basic sites on mesoporous silicas. Nevertheless, two difficulties hinder the application of such a nice method when mesoporous silicas are used as hosts. The first difficulty is the decomposition of base precursor by the thermal approach. Only a small number of

$LiNO_3$ is decomposed on pristine SBA-15 at 400 °C. The increase of temperature to 600 °C can result in the decomposition of $LiNO_3$, whereas such a high temperature accelerates the reaction of strongly basic species with siliceous frameworks. The second difficulty is the poor alkali-resistant ability of silica, which is different from some well-known hosts for solid strong bases such as zirconia and alumina. Mesoporous structure can be destroyed completely due to the reaction between strongly basic species and siliceous frameworks. Therefore, it is hard to generate strong basicity on mesoporous silicas by use of the traditional method.

To overcome both difficulties in the formation of strong basicity on mesoporous silicas, a new strategy was developed by using multifunction of a carbon interlayer, in the present study. A layer of carbon was precoated on mesoporous silica SBA-15 prior to the introduction of base precursor $LiNO_3$. The carbon layer performs two functions in the fabrication of mesoporous strong bases. First, such a carbon layer tailors the surface nature of mesoporous silica and endows the host with reducibility. The base precursor can thus be converted to strongly basic sites through the guest−host redox reaction, which breaks the tradition of thermally induced decomposition. By utilizing the strategy, the temperature for basicity formation is significantly decreased and the conversion of precursor to basic sites is as high as 100%. Second, the carbon layer improves the alkali-resistant ability of mesoporous silica. After the redox reaction of carbon with base precursor, the residual carbon layer prevents the siliceous frameworks from corroding by the formed strongly basic species. As a result, a new kind of material possessing both ordered mesostructure and strong basicity is successfully fabricated.

To study the pathway for the redox conversion of $LiNO_3$, gaseous products formed in the process were analyzed by MS (Figure 2). The signals with m/z values of 30, 32, 44, and 46 were detected and can be ascribed to NO, O_2, CO_2, and NO_2, respectively. The decomposition of $LiNO_3$ on pristine SBA-15 mainly produces NO and O_2 accompanied by a tiny number of NO_2. Interestingly, the conversion of $LiNO_3$ proceeds through a quite different way in the presence of a carbon layer. Gaseous compounds NO and CO_2 are detected as the products. By combining these MS results with the above-mentioned XRD data, the conversion of $LiNO_3$ on pristine SBA-15 and carbon-coated SBA-15 can be described, respectively, by eqs 1 and 2:

$$2LiNO_3 + 2SiO_2 \rightarrow Li_2Si_2O_5 + NO(\uparrow) + NO_2(\uparrow) + O_2(\uparrow) \quad (1)$$

$$4LiNO_3 + 3C \rightarrow 2Li_2O + 4NO(\uparrow) + 3CO_2(\uparrow) \quad (2)$$

As shown in TG curves, the weight losses initiated at about 200 °C can be attributed to the conversion of $LiNO_3$. In the case of LiS, the weight loss derived from $LiNO_3$ conversion is 15.8 wt %, which is in good agreement with the theoretical value calculated by eq 1 (15.7 wt %). The weight loss of LiCS(8) stemmed from $LiNO_3$ conversion is 19.6 wt %, as can be seen from Figure 2. In view of that the support CS(8) itself gives a weight loss of 1.6 wt % in the heating process (Figure S6, Supporting Information), the weight loss derived from the reaction of $LiNO_3$ with carbon should be 18.0 wt %, which is in accord with the theoretical value (18.3 wt %). This verifies the pathway of redox conversion of $LiNO_3$ shown in eq 2. On the basis of the above-mentioned analysis, it is justified that the redox reaction of precursor with carbon interlayer results in the conversion of $LiNO_3$ at low temperatures.

It should be stated that the amount of carbon is of great importance for the formation of strong basicity and the protection of mesostructure. Aiming to convert all of the $LiNO_3$ in the samples (20 wt %), a minimum carbon content of 4.2 wt % is required, which includes 2.6 wt % of carbon that reacted with $LiNO_3$ and 1.6 wt % of carbon that was lost in the synthetic process. It is reasonable that only part of $LiNO_3$ is converted in LiCS(2) and LiCS(4), since the carbon content of both samples is lower than 4.2 wt %. In addition, the destruction of mesostructure is still unavoidable for the samples with low carbon contents, due to the reaction of strongly basic species with exposed siliceous frameworks that is uncovered by carbon. This can explain why the sample LiCS(2)-400 presents a bimodal pore size distribution.

Despite the fact that great efforts have been devoted, the generation of strong basicity on mesoporous silica remains a challenge until now. In the present study, we developed a strategy to overcome both weaknesses of mesoporous silicas by utilizing multifunction of the carbon layer. The carbon interlayer not only promotes the conversion of precursor to basic sites at low temperatures but also prevents the siliceous host from destruction by the newly generated basic species. Hence, ordered mesoporous materials with strong basicity were successfully fabricated, which is highly expected for catalysis and unlikely to be realized by conventional methods. In comparison with traditional methods for synthesis of mesoporous basic materials (e.g., nitrogen incorporation and basic organic groups grafting), our strategy provides an effective method to generate much stronger basicity on mesoporous silicas. Such a strategy may open an avenue for design and synthesis of new functional materials.

CONCLUSIONS

A new strategy was developed to fabricate strong basicity on mesoporous silica by precoating a carbon layer before the introduction of base precursor ($LiNO_3$). The carbon interlayer plays a double role and overcomes both weaknesses of mesoporous silica. On the one hand, the carbon interlayer endows the host with reducing ability. The complete conversion of base precursor can be thus realized at a low temperature via the guest−host redox reaction, which breaks the tradition of thermally induced decomposition that usually requires much higher temperatures. On the other hand, the alkali-resistance of siliceous host is significantly improved due to the carbon interlayer, and the mesostructure can be well preserved after the formation of strongly basic sites. The obtained materials are highly active in the catalytic synthesis of DMC through transesterification and are much superior to the materials without carbon.

ASSOCIATED CONTENT

Supporting Information

Low-angle XRD patterns, IR, TG, and N_2 adsorption−desorption data of carbon-coated samples. This material is available free of charge via the Internet at http://pubs.acs.org.

AUTHOR INFORMATION

Corresponding Authors

*E-mail: lbsun@njut.edu.cn.
*E-mail: liuxq@njut.edu.cn.

Notes

The authors declare no competing financial interest.

■ ACKNOWLEDGMENTS

We acknowledge financial support of this work by the Distinguished Youth Foundation of Jiangsu Province (BK20130045), the National Science Foundation of China (21006048), the National Basic Research Program of China (2013CB733504), China Postdoctoral Science Foundation (20110491406), Jiangsu Planned Projects for Postdoctoral Research Funds (1101155C), and the Project of Priority Academic Program Development of Jiangsu Higher Education Institutions.

■ REFERENCES

(1) Raytchev, P. D.; Bendjeriou, A.; Dutasta, J.-P.; Martinez, A.; Dufaud, V. *Adv. Synth. Catal.* **2011**, *353*, 2067−2077.
(2) Busca, G. *Chem. Rev.* **2010**, *110*, 2217−2249.
(3) Liu, X.-Y.; Sun, L.-B.; Lu, F.; Li, T.-T.; Liu, X.-Q. *J. Mater. Chem. A* **2013**, *1*, 1623.
(4) Ono, Y. *J. Catal.* **2003**, *216*, 406−415.
(5) Corma, A. *Chem. Rev.* **1997**, *97*, 2373−2419.
(6) Jin, X.; Balasubramanian, V. V.; Selvan, S. T.; Sawant, D. P.; Chari, M. A.; Lu, G. Q.; Vinu, A. *Angew. Chem., Int. Ed.* **2009**, *48*, 7884−7887.
(7) Liu, F.; Li, W.; Sun, Q.; Zhu, L.; Meng, X.; Guo, Y.-H.; Xiao, F.-S. *ChemSusChem* **2011**, *4*, 1059−1062.
(8) Wu, G.; Jiang, S.; Li, L.; Guan, N. *Appl. Catal., A* **2011**, *391*, 225−233.
(9) Kresge, C. T.; Leonowicz, M. E.; Roth, W. J.; Vartuli, J. C.; Beck, J. S. *Nature* **1992**, *359*, 710−712.
(10) Zhao, D. Y.; Feng, J. L.; Huo, Q. S.; Melosh, N.; Fredrickson, G. H.; Chmelka, B. F.; Stucky, G. D. *Science* **1998**, *279*, 548−552.
(11) Asefa, T.; MacLachlan, M. J.; Coombs, N.; Ozin, G. A. *Nature* **1999**, *402*, 867−871.
(12) Kim, S. S.; Zhang, W. Z.; Pinnavaia, T. J. *Science* **1998**, *282*, 1302−1305.
(13) Deng, Y.; Wei, J.; Sun, Z.; Zhao, D. *Chem. Soc. Rev.* **2013**, *42*, 4054−4070.
(14) Yang, P.; Zhao, D.; Margolese, D. I.; Chmelka, B. F.; Stucky, G. D. *Nature* **1998**, *396*, 152−155.
(15) Zhang, Z.; Pinnavaia, T. J. *J. Am. Chem. Soc.* **2002**, *124*, 12294−12301.
(16) Cai, W.; Yu, J.; Anand, C.; Vinu, A.; Jaroniec, M. *Chem. Mater.* **2011**, *23*, 1147−1157.
(17) Li, T.-T.; Sun, L.-B.; Liu, X.-Y.; Sun, Y.-H.; Song, X.-L.; Liu, X.-Q. *Chem. Commun.* **2012**, *48*, 6423−6425.
(18) Komura, K.; Mishima, Y.; Koketsu, M. *Appl. Catal., A* **2012**, *445*, 128−132.
(19) Dufaud, V.; Davis, M. E. *J. Am. Chem. Soc.* **2003**, *125*, 9403−9413.
(20) Melero, J. A.; van Grieken, R.; Morales, G. *Chem. Rev.* **2006**, *106*, 3790−3812.
(21) Saravanamurugan, S.; Sujandi; Han, D.-S.; Koo, J.-B.; Park, S.-E. *Catal. Commun.* **2008**, *9*, 158−163.
(22) Chen, S. Y.; Huang, C. Y.; Yokoi, T.; Tang, C. Y.; Huang, S. J.; Lee, J. J.; Chan, J. C. C.; Tatsumi, T.; Cheng, S. *J. Mater. Chem.* **2012**, *22*, 2233−2243.
(23) Xie, Y.; Sharma, K. K.; Anan, A.; Wang, G.; Biradar, A. V.; Asefa, T. *J. Catal.* **2009**, *265*, 131−140.
(24) Wang, T.; Wu, G.; Guan, N.; Li, L. *Microporous Mesoporous Mater.* **2012**, *148*, 184−190.
(25) Xia, Y. D.; Mokaya, R. *Angew. Chem., Int. Ed.* **2003**, *42*, 2639−2644.
(26) Xia, Y. D.; Mokaya, R. *J. Mater. Chem.* **2004**, *14*, 2507−2515.
(27) Sugino, K.; Oya, N.; Yoshie, N.; Ogura, M. *J. Am. Chem. Soc.* **2011**, *133*, 20030−20032.
(28) Kaskel, S.; Schlichte, K. *J. Catal.* **2001**, *201*, 270−274.
(29) Sun, L. B.; Gu, F. N.; Chun, Y.; Yang, J.; Wang, Y.; Zhu, J. H. *J. Phys. Chem. C* **2008**, *112*, 4978−4985.
(30) Sun, L.; Wu, Z.; Kou, J.; Chun, Y.; Wang, Y.; Zhu, J.; Zou, Z. *Chin. J. Catal.* **2006**, *27*, 725−731.
(31) Sun, L. B.; Kou, J. H.; Chun, Y.; Yang, J.; Gu, F. N.; Wang, Y.; Zhu, J. H.; Zou, Z. G. *Inorg. Chem.* **2008**, *47*, 4199−4208.
(32) Sun, L. B.; Gong, L.; Liu, X. Q.; Gu, F. N.; Chun, Y.; Zhu, J. H. *Catal. Lett.* **2009**, *132*, 218−224.
(33) Liu, X.-Y.; Sun, L.-B.; Lu, F.; Liu, X.-D.; Liu, X.-Q. *Chem. Commun.* **2013**, *49*, 8087−8089.
(34) Jiang, W.-J.; Yin, Y.; Liu, X.-Q.; Yin, X.-Q.; Shi, Y.-Q.; Sun, L.-B. *J. Am. Chem. Soc.* **2013**, *135*, 8137−8140.
(35) Sun, L.-B.; Li, J.-R.; Lu, W.; Gu, Z.-Y.; Luo, Z.; Zhou, H.-C. *J. Am. Chem. Soc.* **2012**, *134*, 15923−15928.
(36) Kruk, M.; Jaroniec, M.; Kim, T.-W.; Ryoo, R. *Chem. Mater.* **2003**, *15*, 2815−2823.
(37) Kruk, M.; Jaroniec, M. *Chem. Mater.* **2001**, *13*, 3169−3183.
(38) Jaroniec, M.; Solovyov, L. A. *Langmuir* **2006**, *22*, 6757−6760.
(39) Sun, L.-B.; Tian, W.-H.; Liu, X.-Q. *J. Phys. Chem. C* **2009**, *113*, 19172−19178.
(40) Sun, Y.-H.; Sun, L.-B.; Li, T.-T.; Liu, X.-Q. *J. Phys. Chem. C* **2010**, *114*, 18988−18995.
(41) Gong, L.; Sun, L.-B.; Sun, Y.-H.; Li, T.-T.; Liu, X.-Q. *J. Phys. Chem. C* **2011**, *115*, 11633−11640.
(42) Yin, Y.; Jiang, W.-J.; Liu, X.-Q.; Li, Y.-H.; Sun, L.-B. *J. Mater. Chem.* **2012**, *22*, 18514−18521.
(43) Tian, W.-H.; Sun, L.-B.; Song, X.-L.; Liu, X.-Q.; Yin, Y.; He, G.-S. *Langmuir* **2010**, *26*, 17398−17404.
(44) Sun, L. B.; Yang, J.; Kou, J. H.; Gu, F. N.; Chun, Y.; Wang, Y.; Zhu, J. H.; Zou, Z. G. *Angew. Chem., Int. Ed.* **2008**, *47*, 3418−3421.
(45) Krishnan, C. K.; Hayashi, T.; Ogura, M. *Adv. Mater.* **2008**, *20*, 2131−2136.
(46) Li, T.-T.; Sun, L.-B.; Gong, L.; Liu, X.-Y.; Liu, X.-Q. *J. Mol. Catal. A: Chem.* **2012**, *352*, 38−44.
(47) Liu, S.; Ma, J.; Guan, L.; Li, J.; Wei, W.; Sun, Y. *Microporous Mesoporous Mater.* **2009**, *117*, 466−471.
(48) Honda, M.; Suzuki, A.; Noorjahan, B.; Fujimoto, K.-i.; Suzuki, K.; Tomishige, K. *Chem. Commun.* **2009**, 4596−4598.
(49) Stoica, G.; Abelló, S.; Pérez-Ramírez, J. *ChemSusChem* **2009**, *2*, 301−304.